



**13<sup>th</sup> World Conference on Earthquake Engineering**  
**Vancouver, B.C., Canada**  
**August 1-6, 2004**  
**Paper No. 3016**

## **SOLUTIONS FOR MITIGATING SOIL LIQUEFACTION EFFECTS A NUMERICAL STUDY**

**AHMAD JAFARI MEHRABADI<sup>1</sup> AND RADU POPESCU<sup>2</sup>**

### **SUMMARY**

A large number of the observed disastrous effects during past earthquakes, including loss of human life and severe damages to many structures, are related to soil failure or occurrence of large displacements caused by soil liquefaction. Due to man-made activities and nature of the soil, Fraser River Delta in British Columbia is highly vulnerable to liquefaction hazards, and, annually, a large amount of funds is allotted to mitigate the detrimental consequences of the soil liquefaction in this region. In this respect, an initiative has been introduced by NSERC to optimize the required remediation measures in the Fraser River Delta by means of numerical simulations and centrifuge experiments.

This paper presents part of class "A" predictions, i.e. numerical results obtained before performing the relevant experiments, for the first centrifuge test planned for the NSERC initiative. A multi-yield constitutive model implemented in the finite element program Dynaflo is used to predict the soil behavior under seismic loading. The paper will present the constitutive model calibration procedure and the results of the class A prediction. The purpose of this study is to validate the proposed numerical model and use it for extending the scope of the centrifuge experimental program.

### **INTRODUCTION**

Liquefaction induced displacements during past earthquakes have caused severe damages to many structures resulting in loss of human life and drastic financial burdens. To reduce the risk of soil failure due to this phenomenon soil improvement techniques should be taken into account. Optimization of such remediation methods, i.e., great savings in funds without losing the effectiveness of the soil improvement measures, is highly desirable. Due to man-made activities and the nature of the soil in the Fraser River Delta in British Columbia, this region is highly vulnerable to liquefaction hazards. In this regard, NSERC sponsors research to optimize the required mitigation measures against liquefaction for the Fraser River Delta by means of centrifuge experiments and numerical modeling. The NSERC sponsored liquefaction remediation initiative (LRI) includes soil laboratory testing, numerical modeling and centrifuge experiments

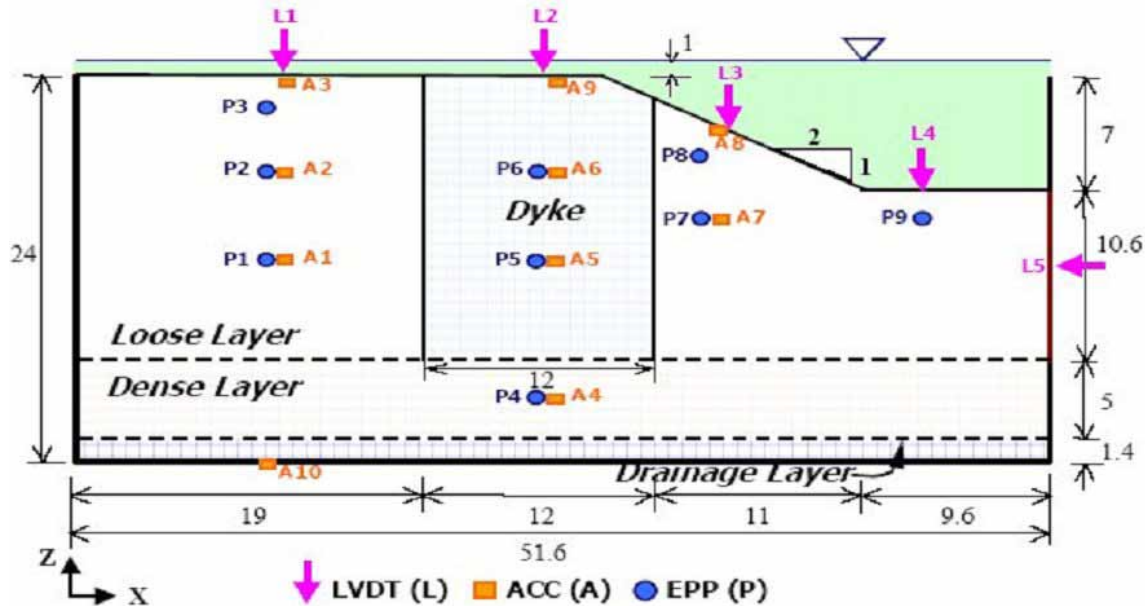
---

<sup>1</sup> Ph.D. candidate, Memorial University of Newfoundland, St. John's, NL, Canada, Email: [ahmad@engr.mun.ca](mailto:ahmad@engr.mun.ca)

<sup>2</sup> Associate Professor, Memorial University of Newfoundland, Email: [radu@engr.mun.ca](mailto:radu@engr.mun.ca)

to evaluate the performance of various soil liquefaction countermeasures. The primary goal of LRI is to optimize soil improvement methods for liquefaction hazards. Immediate benefits of this study include great saving in amount and extent of soil treatment projects, and in the long run it results in saving of lives as well as minimizing damages in the event of a major earthquake. Soil laboratory testing and part of numerical modeling are performed at UBC. C-CORE is responsible for conducting centrifuge experiments, and MUN provides additional numerical modeling. In addition, non-academic partners such as consulting firms have joined this initiative to provide the soil conditions and types of the structures that have priority to be studied. They will also review the centrifuge data and numerical analyses. The recommended base model to be studied is an earth slope made of Fraser River sand, and eight centrifuge tests with different mitigation configurations and two different acceleration time histories will be conducted in the framework of LRI.

The NSERC liquefaction remediation initiative includes eight centrifuge tests. These tests will be conducted on an earth slope as shown in Figure 1 [1]. In this Figure EPP, LVDT and ACC are pore water pressure transducer, linear variable differential transducer and accelerometer, respectively. The earthquake records considered for the centrifuge experiments are related to the two levels of risk proposed for Vancouver area, i.e., 10% probability of occurrence and 2% probability of occurrence in a 50-year period related to the events A475 and A2475, respectively, as shown in Figure 2 (see [1] and [2]).



| Test Number | Test Configuration                                    | EQ event  |
|-------------|---|---|
| CT1         | Loose sand layer, No ground improvement               | A475 <sup>(i)</sup> followed by A2475 <sup>(ii)</sup> |
| CT2         | Loose sand layer, No ground improvement               | A2475   |
| CT3         | Loose sand layer with dense dyke                      | A475 followed by A2475                                |
| CT4         | Loose sand layer with drainage dyke                   | A475 followed by A2475                                |
| CT5         | Loose sand layer with barrier layer                   | A475 followed by A2475                                |
| CT6         | Loose sand layer with barrier layer and drainage dyke | A475 followed by A2475                                |
| CT7 & CT8   | TBA   | A475 followed by A2475                                |

(i) A475 is a 10% possibility within 50 yrs.  
(ii) A2475 is a 2% possibility within 50 yrs.

**Fig.1** General layout of the centrifuge tests [1]

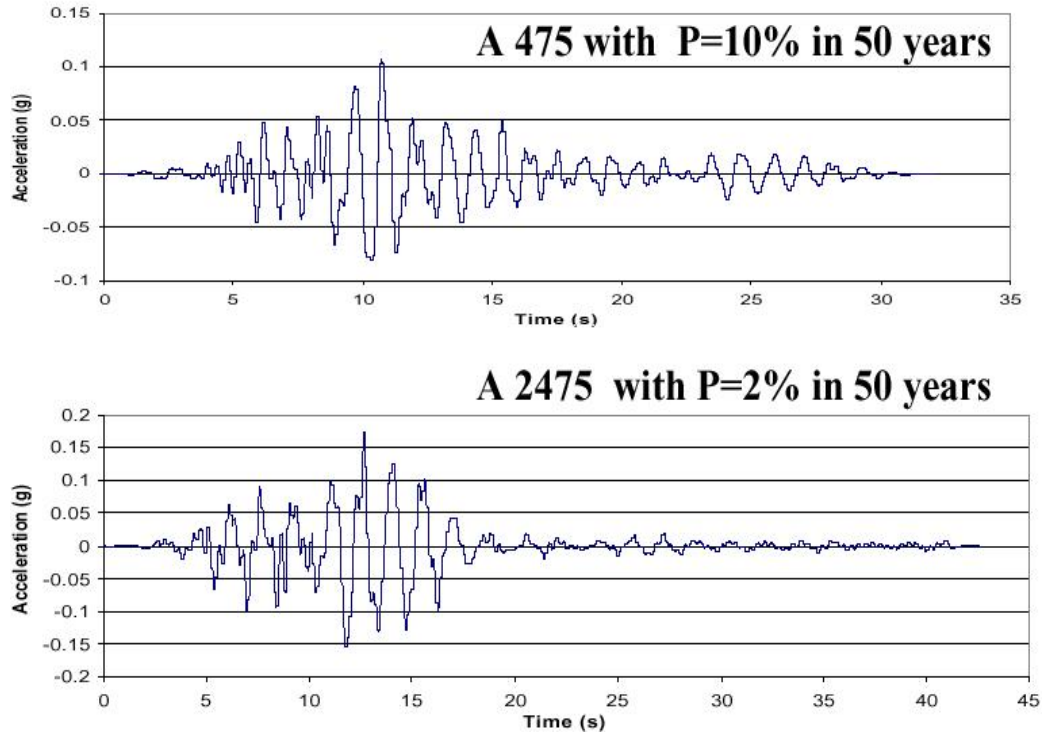


**Fig.2** Acceleration time histories used in the centrifuge tests (From [1] and [2])

## MULTI-YIELD PLASTICITY SOIL CONSTITUTIVE MODEL

The constitutive model used in this study is the multi-yield plasticity soil constitutive model implemented in the finite element code Dynaflow. This model has been validated several times in the past for analysis of liquefaction phenomenon [3]. The model is a kinematic hardening model based on a relatively simple plasticity theory [4], and is applicable to both cohesive and cohesionless soils. Fundamental theory behind the model has originated from the concept of a “field of work-hardening moduli” [5] by approximating the nonlinear elastic plastic stress-strain curve into a number of linear segments with constant shear moduli. This results in defining a series of nested yield surfaces in the stress space. Each yield surface corresponds to a region of a constant shear modulus. The outermost surface is related to zero shear modulus, and is called failure surface. Both Drucker-Prager and Mohr-Coulomb type surfaces can be employed in the model for frictional materials (sands).

The plastic potential is assumed to be associative for its deviatoric component and non-associative for its dilatational (volumetric) component. The volumetric component is defined based on mobilized stress ratio to account for dependence of soil dilatational behavior on the mobilized stress ratio. The soil hysteretic behavior and shear stress-induced anisotropic effects are simulated by a purely deviatoric kinematic hardening rule [6]. Main features of the multi-yield plasticity soil constitutive model are shown in Figure 3[7]. The constitutive parameters of the multi-yield soil plasticity model are shown in Table 1.

## CALIBRATION OF THE NUMERICAL MODEL FOR FRASER RIVER SAND

The procedure for calibrating the numerical model for loose Fraser River sand with relative density of 40% is presented hereafter.

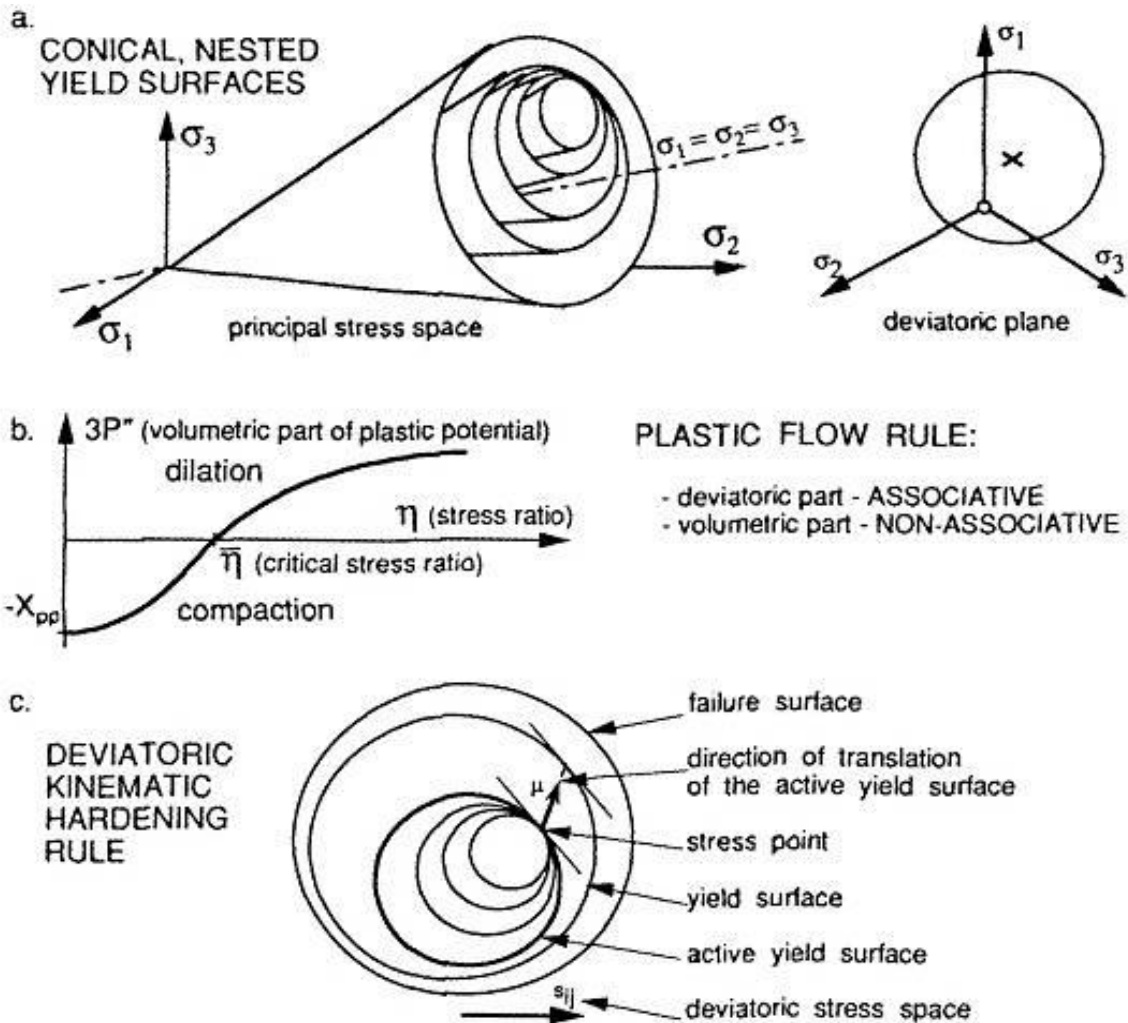


Fig. 3 Main features of the multi-yield Plasticity soil model (Curtailed from [7])

### I- State parameters

According to the recent laboratory tests at UBC [1] the index parameters and hydraulic conductivity of the Fraser River sand are as follows.

|  |                        |
|--|------------------------|
| $e_{\max} = 0.94$                          | Maximum void ratio     |
| $e_{\min} = 0.62$                          | Minimum void ratio     |
| $\rho_s = 2710 \text{ (kg/m}^3\text{)}$    | Mass density           |
| $k = 0.044 \text{ (cm/s)}$ at $D_r = 36\%$ | Hydraulic conductivity |

Void ratio and porosity can be obtained from equations 1 and 2. Also, the value of hydraulic conductivity can be corrected for  $D_r = 40\%$  based on Kozeny-Carman relationship [8], i.e., expressing variation of permeability with void ratio as shown in relationship 3.

$$D_r = \frac{e_{\max} - e}{e_{\max} - e_{\min}} \quad (1)$$

$$n^w = \frac{e}{1+e} \quad (2)$$

$$k \propto \frac{e^3}{1+e} \quad (\text{Based on Kozeny-Carman relationship}) \quad (3)$$

The above relationships leads to the following values for state parameters of the loose Fraser River sand.

|                            |                        |
|----------------------------|------------------------|
| $n^w = 0.448$              | Porosity               |
| $k = 0.042 \text{ (cm/s)}$ | Hydraulic conductivity |

## II-Low-strain elastic parameters:

The parameters  $p_0$ , and  $\nu$  are chosen as follows.

$p_0 = 100 \text{ (KPa)}$  A reference effective mean normal stress

$\nu = 0.3$  A typical value for sand

Power exponent,  $n$ , is used to estimate the values of shear modulus ( $G$ ) at different effective mean normal stress levels ( $p$ ), most commonly by means of the following formula [9].

$$G = \left(\frac{p}{p_0}\right)^n G_0 \quad (4)$$

The most commonly accepted value for  $n$  is 0.5 [10]. The low-strain shear modulus of Fraser River sand with  $D_r = 30\%$  at a reference pressure equal to 200 KPa can be found in literature based on the results of isotropically consolidated drained triaxial test [11].

$G_{sec} = 39 \text{ MPa}$  At a shear strain level=0.05%

At a reference stress equivalent to 100 KPa, the shear modulus can be estimated using equation 4:

$$(G_{sec})_{100} = \left(\frac{100}{200}\right)^{0.5} \cdot (G_{sec})_{200} = 27.58 \text{ MPa}$$

For correction of the shear modulus with relative density, a relationship between shear modulus and void ratio is required. In this regard, available correlation formulas may be used. Although, most of the available correlations have been obtained for a very low strain level (mostly based on resonant column tests), since they are functions of void ratio, they can give a sense regarding the variation of modulus due to changes in void ratio. For instance, based on correlations suggested by Hardin and Richard [12], and Bellotti [13], it is inferred that:

$$G_0 \propto \frac{(2.97 - e)^2}{1 + e} \quad \text{Hardin and Richard} \quad (5)$$

$$G_0 \propto \exp(1.39D_r) \quad \text{Bellotti} \quad (6)$$

Using these relationships the following values can be obtained for the shear modulus of Fraser River sand at  $D_r = 40\%$ .

|                               |                    |
|-------------------------------|--------------------|
| $G_{sec} = 28.83 \text{ MPa}$ | Hardin and Richard |
|-------------------------------|--------------------|

|                              |          |
|------------------------------|----------|
| $G_{sec} = 31.6 \text{ MPa}$ | Bellotti |
|------------------------------|----------|

It seems that a combination of correlation formulas and the available test suggests a value around 30 MPa for low (strain shear modulus of Fraser River sand ( $D_r = 40\%$ )).

### III-Yield parameters:

There is no available report mentioning the exact value of the friction angle for Fraser River sand at  $D_r = 40\%$ . The values obtained from literature based on the results of monotonic triaxial tests performed on very loose Fraser River sand with relative density of about 20% are about  $36^\circ$  (Vaid et al. 2001[14]); The correlation suggested by USACE (1992)[15], gives a value of about  $35^\circ$  for friction angle of Fraser River sand based on its relative density, grain size, and gradation. In another attempt, a correlation formula suggested by Hanna [16], based on the results of the conventional triaxial compression tests, Rowe's dilatancy theory, and assuming a phase transformation angle equivalent to  $34^\circ$  [14], a value of  $39.8^\circ$  can be obtained for plane-strain friction angle (about  $36^\circ$  in triaxial condition [17]) of the Fraser River sand.

As it can be understood from the above discussion, the available data for the friction angle of Fraser River sand are very scattered. Here, a value of  $36^\circ$  is adopted for the friction angle of Fraser River sand both in compression and in extension. This value is very close to the results of correlation formulas and experience with similar sands. The coefficient of lateral earth pressure at rest is estimated from the theory of elasticity for plane strain condition.

$$k_0 = \frac{\nu}{1 - \nu} = \frac{0.3}{1 - 0.3} = 0.43$$

Regarding the maximum shear strain at failure for Fraser River sand, only qualitative information can be obtained from the available tests found in the literature and the results of the monotonic simple shear test conducted at UBC. The following values, within the range of the values for similar sands, are selected.

$$(\epsilon_{dev}^{max})_c = 0.08 \quad \text{Maximum shear strain in compression}$$

$$(\epsilon_{dev}^{max})_E = 0.08 \quad \text{Maximum shear strain in extension.}$$

### IV-Dilation parameters:

The value of dilation angle (phase transformation angle), is a material property, and is independent of loading mode, type of deformation, and relative density [14]. This angle for Fraser River sand, obtained from laboratory tests at different conditions, is a constant value of about  $34^\circ$  [14]. The dilation parameter  $X_{pp}$  is estimated by performing liquefaction strength analysis. Liquefaction strength analysis is based on back-fitting the experimental liquefaction strength curve using finite element simulations of cyclic undrained triaxial or simple shear tests [18]. Cyclic undrained simple shear tests with and without initial static shear stress have been recently performed at UBC on Fraser River sand samples. The tests without initial static shear are used here to estimate the value of the dilation parameter  $X_{pp}$  for this sand. Figure 4 shows the liquefaction strength curve obtained from the UBC tests and the results of back-fitting of these curves using numerical simulations. A value of  $X_{pp}=0.48$  can reasonably reproduce the experimental results obtained from the UBC cyclic simple shear tests.

The constitutive parameters estimated for loose Fraser River sand as described before are shown in Table 1. Also, the constitutive parameters for dense ( $D_r = 80\%$ ) sand are shown in that table. The constitutive parameters for dense sand have been obtained using the same methodology discussed in this section.

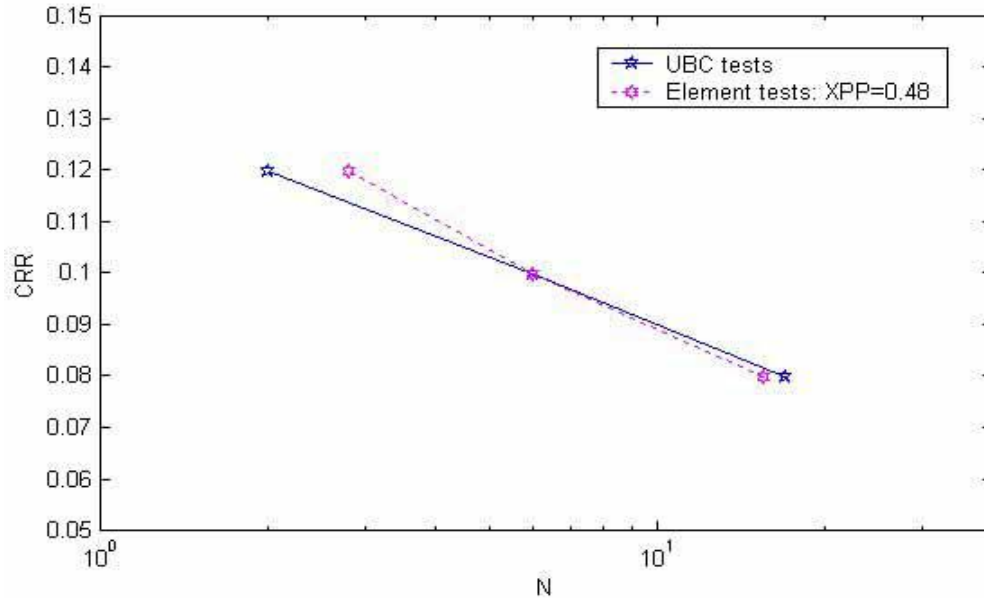


**Fig. 4** Determination of the dilation parameter for loose Fraser River sand using UBC cyclic simple shear tests without initial static shear stress (tests results from [1]) (N is number of cycles to liquefaction, and CRR is cyclic resistance ratio)

| Constitutive parameters of Fraser River sand  | Symbol                    | Values                |                        | Type                |
|---|---------------------------|-----------------------|------------------------|---------------------|
|   |                           | Loose                 | Dense                  |                     |
| Mass density ( $\text{kg/m}^3$ )              | $\rho_s$                  | 2710                  | 2710                   | State Parameters    |
| Porosity                                      | $n^w$                     | 0.448                 | 0.406                  |                     |
| Hydraulic conductivity (permeability) (cm/s)  | $k$                       | 0.042                 | 0.031                  |                     |
| Low-strain shear modulus (Mpa)                | $G_0$                     | 30                    | 52.31                  | Elastic Parameters  |
| Reference effective mean normal stress        | $p_0$                     | 100                   | 100                    |                     |
| Powe exponent                                 | $n$                       | 0.5                   | 0.5                    |                     |
| Poisson ratio                                 | $\nu$                     | 0.3                   | 0.3                    |                     |
| Friction angle at failure                     | $\phi$                    | $36^\circ$            | $42^\circ$             | Yield Parameters    |
| Coefficient of lateral earth pressure at rest | $k_0$                     | 0.43                  | 0.43                   |                     |
| Soil cohesion                                 | $c$                       | 0                     | 0                      |                     |
| Maximum deviatoric strain                     | $\varepsilon_{dev}^{max}$ | 0.08 (C),<br>0.08 (E) | 0.01 (C),<br>0.008 (E) |                     |
| Dilation angle (phase transformation angle)   | $\Psi$                    | $34^\circ$            | $34^\circ$             | Dilation Parameters |
| Dilation parameter                            | $X_{PP}$                  | 0.48                  | 0.01                   |                     |

**Table 1** Constitutive parameters of Fraser River sand (C=Compression; E=Extension)

### CLASS A PREDICTION FOR THE FIRST CENTRIFUGE TEST

In this section the results of numerical class A prediction of the first centrifuge test are briefly presented. These results are related to the centrifuge model with no ground improvement, and earthquake loading is A475 followed by A2475 (i.e. CT1 in Figure 1). The soil constitutive parameters used in this prediction are shown in Table 1. Figure 5 shows the predicted

displacement contours for the prototype scale at the end of two earthquakes. The predicted contours of maximum shear strain are shown in Figure 6. Figure 7 shows the predicted vertical settlement contours at the end of two earthquakes. The predicted contours of excess pore water pressure ratio at two different times are shown in Figure 8. Figures 9 to 13 show the predicted response time histories at different transducers, i.e. LVDT1, LVDT2, EPP3, EPP8, and ACC9, respectively.

A large portion of the slope movement takes place during the event A2475. As indicated in Figure 5, total predicted displacement at slope crest is about 1 m at the end of event A475, while it reaches to 3 m at the end of the second earthquake. The predicted settlement in the free field is about 0.5 m at the end of the event A475, and increases to about 1.4 m at the end of event A2475 (see Figures 7,9 and 10). The time interval between the two earthquake events modeled here allows complete dissipation of the generated pore water pressure during the first event. This is shown in Figures 11 and 12. Initial liquefaction is predicted to occur at shallow depths in the free field during both events, as shown in Figure 11. Below slope, due to static shear and the tendency of soil to dilate, the maximum excess pore pressure ratio is predicted to reach much lower values, as illustrated in Figure 12. The predicted accelerations at slope crest (ACC9) indicate some attenuation in maximum values during the second event due to minor soil softening (Figure 13). Larger attenuations of maximum accelerations have been predicted in the free field where soil was predicted to liquefy (ACC3 – results not shown here)

## **SUMMARY AND CONCLUSION**

A method for calibrating the multi-yield plasticity soil constitutive model was presented in this paper. The soil properties have been estimated based on results of UBC laboratory soil tests, information in the literature and engineering judgment. The dilation parameter has been estimated based on liquefaction strength analysis. Since, none of the centrifuge tests shown in Fig.1 has been performed yet, the predictions presented in this paper are class A predictions, and they will be used to evaluate the performance of the numerical model after conducting the relevant centrifuge experiment. A more detailed set of class A predictions described here can be found at: <http://www.civil.ubc.ca/liquefaction/classamarch04.pdf>. [1]

## **ACKNOWLEDGEMENT**

This research is financially supported by NSERC as a part of a liquefaction remediation initiative and Grant No RG203795-02. This support is gratefully acknowledged. Also, the authors are indebted to Professor J. H. Prevost, for providing the finite element code, Dynaflo, used in this paper.

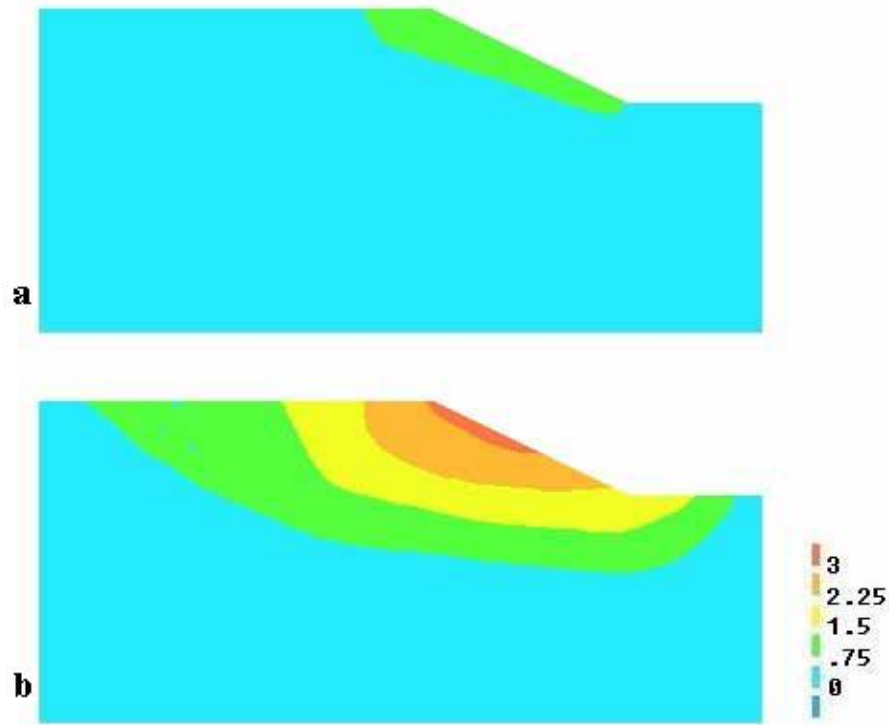


**Fig. 5** Predicted displacements contours  
 (a: End of event A475; b: End of event A2475)

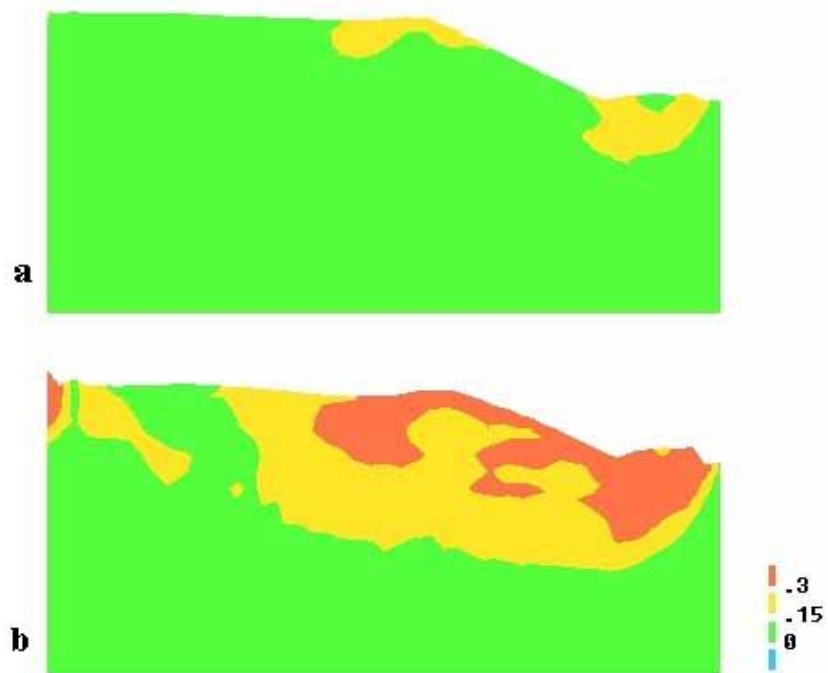


**Fig. 6** Predicted maximum shear strain contours  
 (Deformation magnification factor =1; a: End of event A475 and b: End of event A2475)

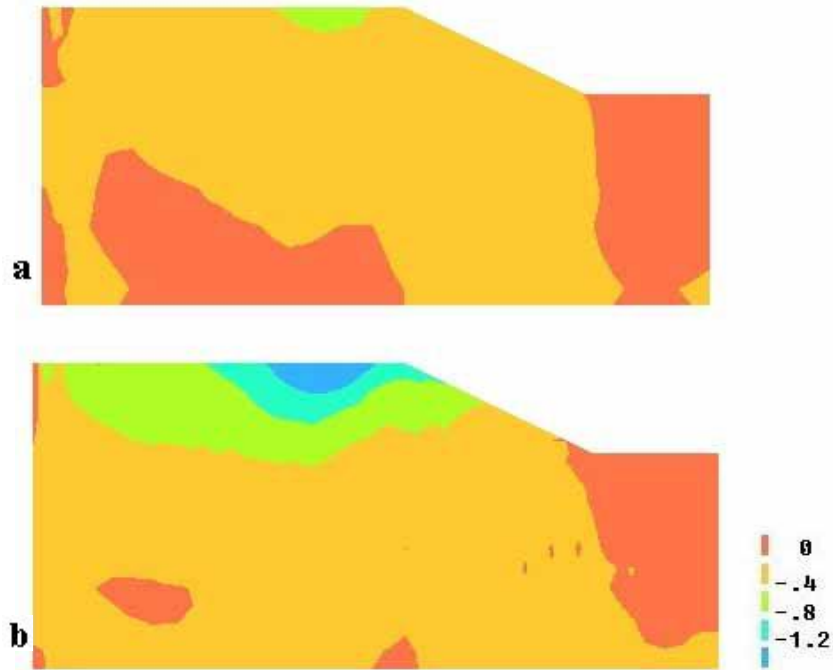


**Fig. 7** Predicted contours of vertical settlement  
(a: End of event A475 and b: End of event A2475)

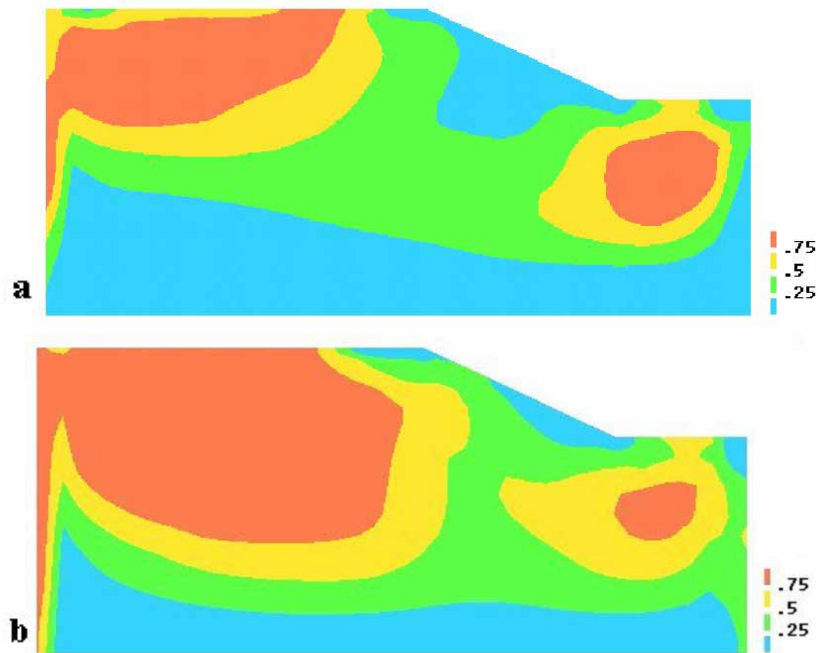


**Fig. 8** Predicted pore pressure ratio at two different times  
(a: 12 s after the beginning of event A475 and b: 17.8 s after the beginning of event A2475)

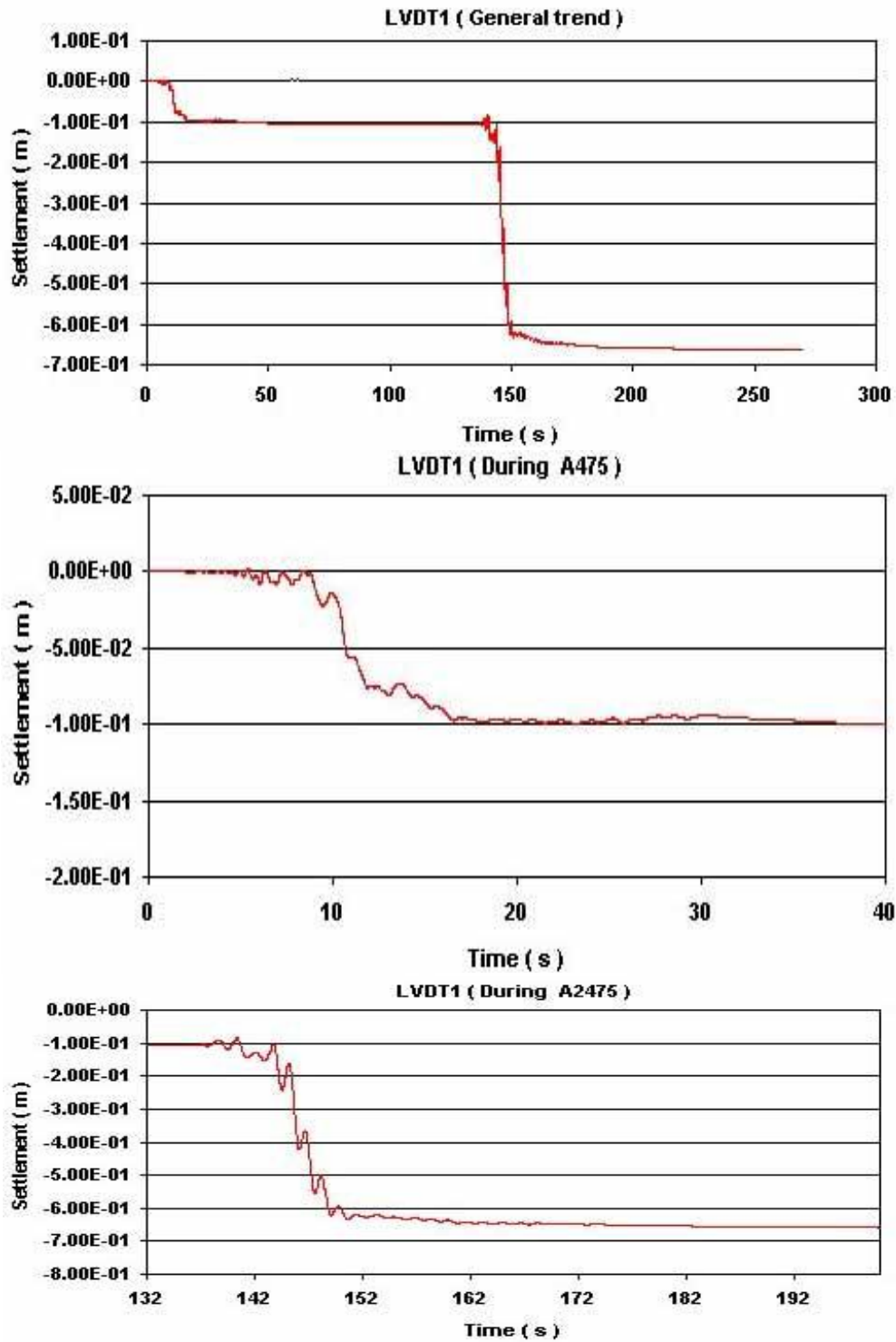
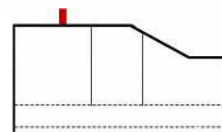


Fig. 9 Predicted vertical displacement time history at LVDT1



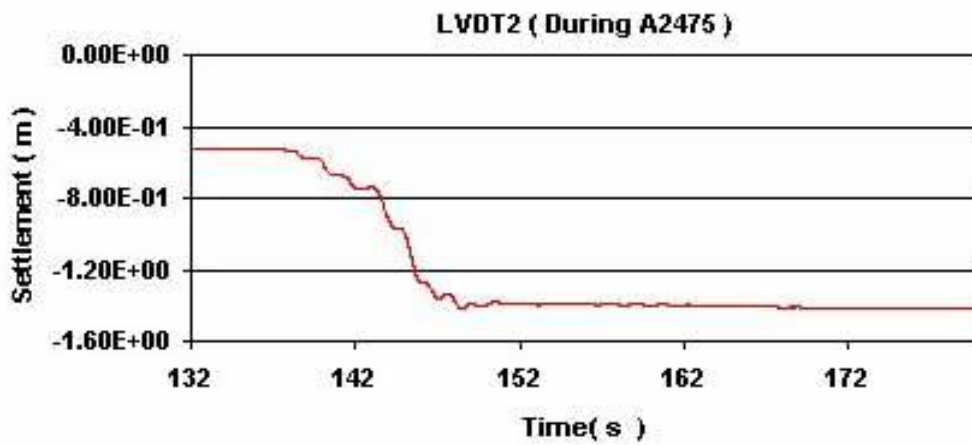
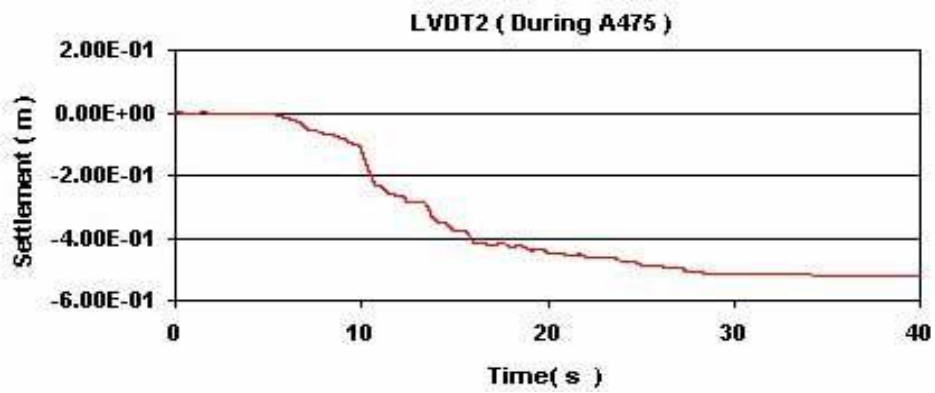
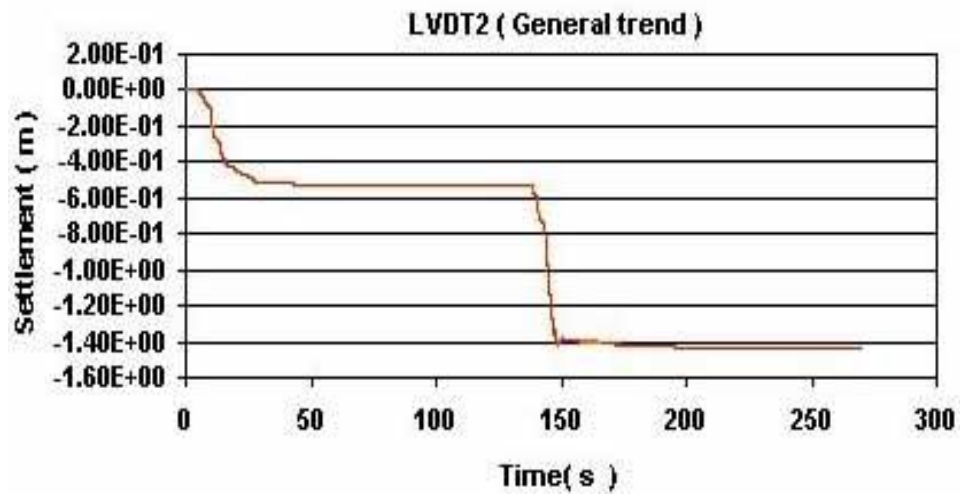
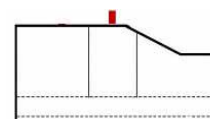


Fig. 10 Predicted vertical displacement time history at LVDT2



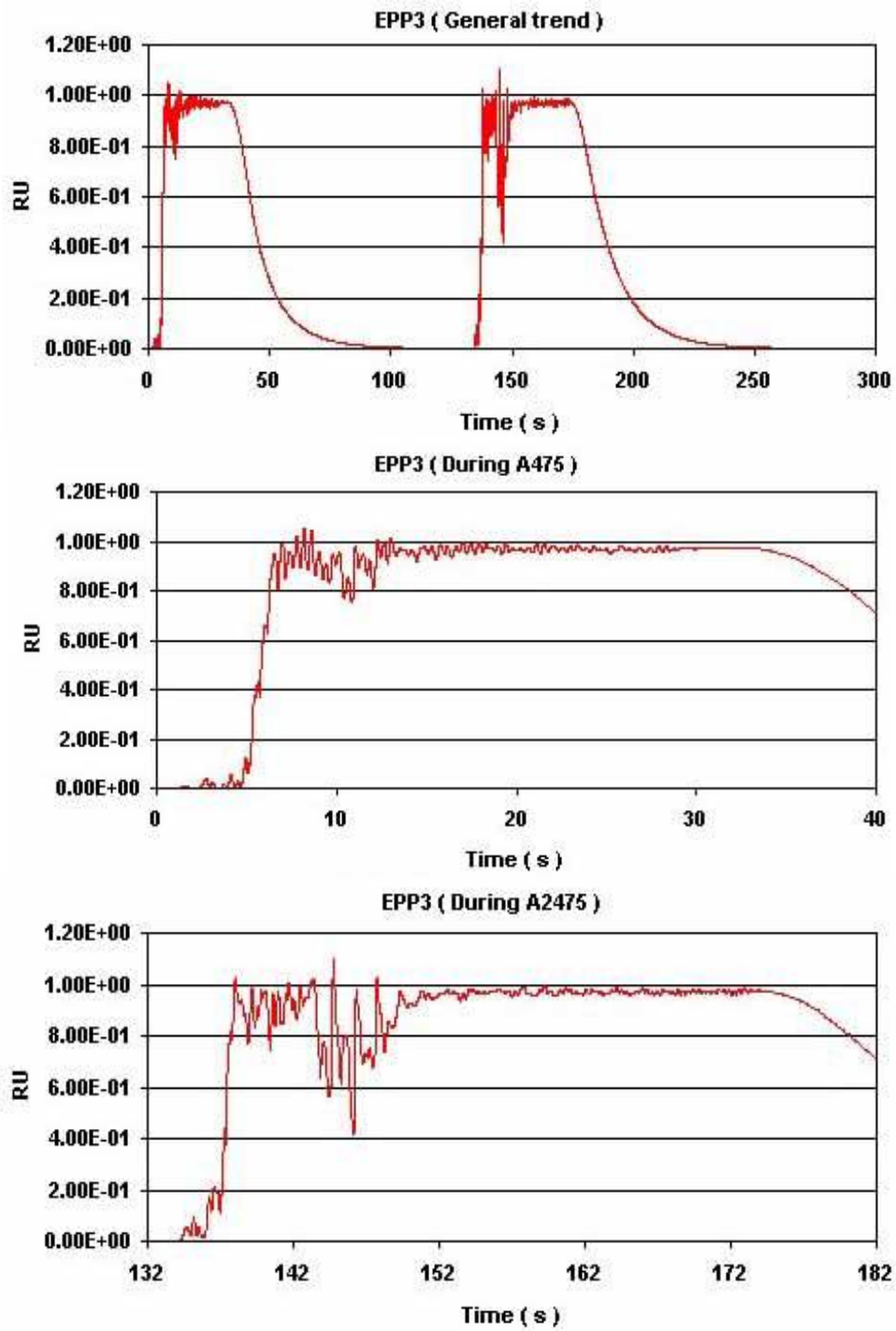


Fig.11 Predicted excess pore water pressure ratio time history at EPP3



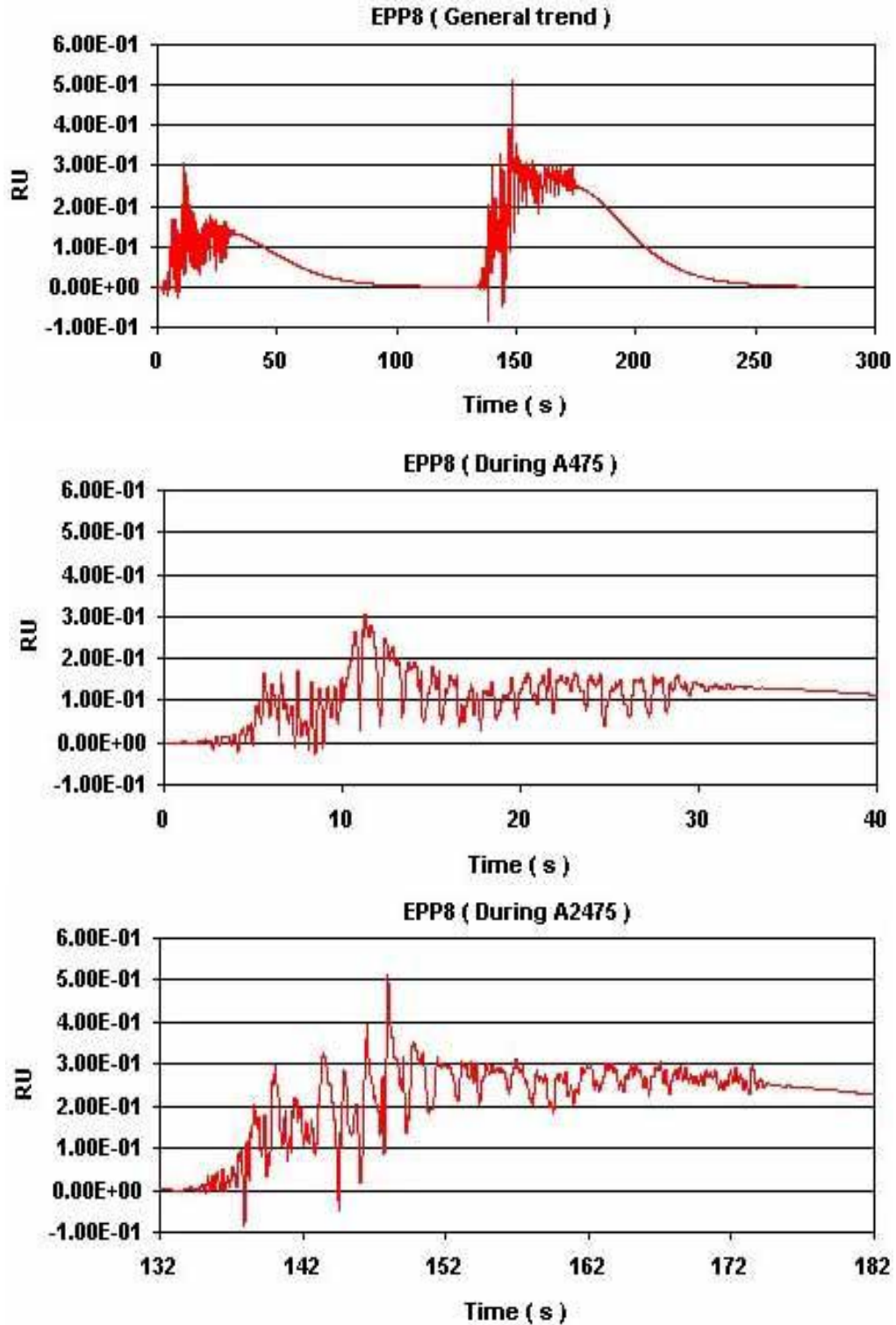
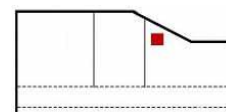


Fig.12 Predicted excess pore water pressure ratio time history at EPP8



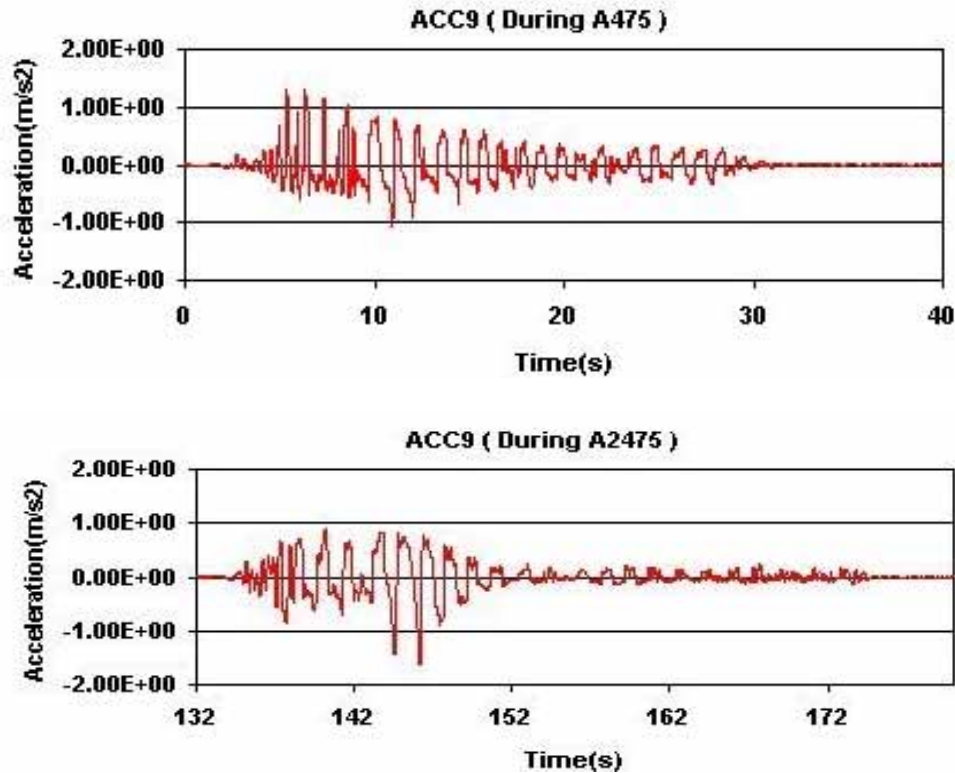
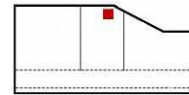


Fig. 13 Predicted acceleration time history at ACC9



## REFERENCES

1. Earthquake Induced Damage Mitigation from Soil Liquefaction website. 2003. Posted at: <http://www.civil.ubc.ca/liquefaction/>.
2. Seid Karbasi, M. 2003. Time Histories of Input Motions Selected for Physical and Numerical Modeling. Report No. 2003/02, Civil Engineering Department of University of British Columbia.
3. Popescu, R., and Prevost, J.H. 1993. Centrifuge validation of a numerical model for dynamic soil liquefaction. *Soil Dynamics and Earthquake Engineering*, 12: 73-90.
4. Prevost, J.H., 1985. A simple plasticity theory for frictional cohesionless soils. *J. Soil Dynam. and Earthq. Eng.*, 4(1): 9-17.
5. Mroz, Z., 1967. On the behavior of anisotropic workhardening. *J. Mech. Phys. Solids*, 15: 163-175
6. Prevost, J.H. 1989. DYNALD, a computer program for nonlinear seismic site response analysis. Technical report NCEER-89-0025. National Center for Earthquake Engineering research. State University of New York at Buffalo.
7. Popescu, R. 1995. Stochastic variability of soil properties: Data Analysis, Digital Simulation, effects on system behavior. Ph.D. Thesis, Princeton University, Princeton, NJ
8. Das, B.M. 1985. Principles of geotechnical engineering. PWS Engineering. Boston.
9. Cubrinovski, M. and Ishihara, K. 1998. Modelling of sand behaviour based on state concept, *Soils and Foundations*, 38(3): 115-127.
10. Kardestuncer, H., and Norrie, D. 1987. Finite element handbook. Mc. Graw-Hill Company.
11. Vaid, Y.P., and Eliadorani, A. 2000. Undrained and drained (?) stress-strain response. *Can. Geotech. J.* 37: 1126-1130.
12. Hardin, B. O., and Richad, F. E. 1963. Elastic wave velocities in granular soils. *Journal of the Soil Mechanics and Foundations Division, ASCE*, 89(SM1): 33-65.

13. Bellotti, R., Ghionna, V., Jamiolkowski, M., Lancellotta, R., and Manfredini, G. 1986. Deformation characteristics of cohesionless soils from in-situ tests. In S.P. Clemence, editor, *Use of In-Situ Tests in Geotechnical Engineering*, pp: 47-73. ASCE, New York.
14. Vaid, Y.P., Stedman, J.D., and Sivathayalan, S. 2001. Confining stress and static shear effects in cyclic liquefaction. *Can. Geotech. J.* 38: 580-591.
15. USACE. 1992. Bearing capacity of soils. E M 1110-1-1905.
16. Hanna, A. 2001. Determination of plane-strain shear strength of sand from the results of triaxial tests. *Can. Geotech. J.* 38: 1231-1240.
17. Kulhawy, F.H. and Mayne, P.W. 1990. Manual on estimating soil properties for foundation design. Final Report 1493-6, EL-6800, Electric Power Research Institute, Palo Alto, CA.
18. Prevost J.H., and Popescu R. 1996. Constitutive relations for soil materials. *Electronic Journal of Geotechnical Engineering*, ASCE, <http://www.ejge.com/1996/Ppr9609/Ppr9609.htm>.